Potential oscillations in a proton exchange membrane fuel cell with a Pd–Pt/C anode

Pietro P. Lopes [a], Edson A. Ticianelli [a], Hamilton Varela [a,b,*]

[a] Instituto de Química de São Carlos, Universidade de São Paulo, C.P. 780, CEP 13560-970, São Carlos, SP, Brazil
[b] Ertl Center for Electrochemistry and Catalysis, GIST, Cheomdan-gwagiro 261, Buk-gu, Gwangju 500-712, South Korea

ARTICLE INFO

ABSTRACT

We report in this paper the occurrence of potential oscillations in a proton exchange membrane fuel cell (PEMFC) with a Pd–Pt/C anode, fed with H_2/100 ppm CO, and operated at 30 °C. We demonstrate that the use of Pd–Pt/C anode enables the emergence of dynamic instabilities in a PEMFC. Oscillations are characterized by the presence of very high oscillation amplitude, *ca.* 0.8 V, which is almost twice that observed in a PEMFC with a Pt–Ru/C anode under similar conditions. The effects of the H_2/CO flow rate and cell current density on the oscillatory dynamics were investigated and the mechanism rationalized in terms of the CO oxidation and adsorption processes. We also discuss the fundamental aspects concerning the operation of a PEMFC under oscillatory regime in terms of the benefit resulting from the higher average power output.

1. Introduction

Fuel cells convert the chemical energy of a fuel such as hydrogen and an oxidant into electricity and heat. When hydrogen production process is made by steam reform of low-weight alcohols, CO is present in the fuel stream at unacceptable levels for a PEMFC equipped with a Pt/C anode [1]. In order to overcome this problem, several strategies have been attempted to eliminate the CO poisoning effect on Pt based electrocatalysts, and the use of Pt bimetallic alloys show the most promising route in this direction [1–4]. Together with the higher CO tolerance feature, bimetallic electrocatalysts such as PtRu might promote rich dynamic behavior such as spontaneous potential oscillations under certain conditions [5,6]. This oscillatory phenomenon have been discussed by Datta and co-workers [5,7] where a reaction mechanism for the hydrogen oxidation reaction (ROH) taking place in the presence of CO can emulate the basic oscillation features. The authors also discuss the higher power generation under oscillatory conditions, suggested as an alternative route to improve the cell efficiency when CO is present.

It has been reported that operating a fuel cell under oscillatory regime might result in an overall higher performance [8]. This is because the oscillatory regime prevents the anode to get completely poisoned by adsorbed carbon monoxide as it is the case under stable non-oscillatory conditions. Instead, the catalyst surface is periodically cleaned as oscillations proceed. Although oscillations have been observed for several electro-oxidation reactions [9–12] carried out in half-cell set-up, there are very few reports of oscillatory behavior in PEMFCs. In all cases, oscillations are found in fuel cells using PtRu/C anodes and fed with H_2/CO mixtures. Moreover, reported oscillations have a strong relaxation feature and amplitudes smaller than 0.5 V [5–7]. In the present paper we report the spontaneous emergence of potential oscillations in a PEMFC with a Pd–Pt/C anode, fed with a H_2/CO (100 ppm) mixture and operated at 30 °C. The effects of the H_2/CO flow rate and cell current density on the oscillatory dynamics were investigated. Mechanistic aspects are rationalized in terms of the CO oxidation and adsorption processes.

2. Materials and methods

The Pd–Pt/C catalyst employed in this study was synthesized by the Wet Impregnation Method [13] of the Pd precursor over a commercial Pt/C (20% E-Tek Inc.). The desired amount of $PdCl_2$ (Alfa Aesar) was dissolved in ultrapure water (Milli-Q) where the Pt/C powder was added. This mixture was kept in an ultra-sound bath for 3 h, than evaporated to dryness in a hot-plate. The obtained

* Corresponding author at: Instituto de Química de São Carlos, Universidade de São Paulo, C.P. 780, CEP 13560-970, São Carlos, SP, Brazil. Tel.: +55 16 33738059; fax: +55 16 33738059.
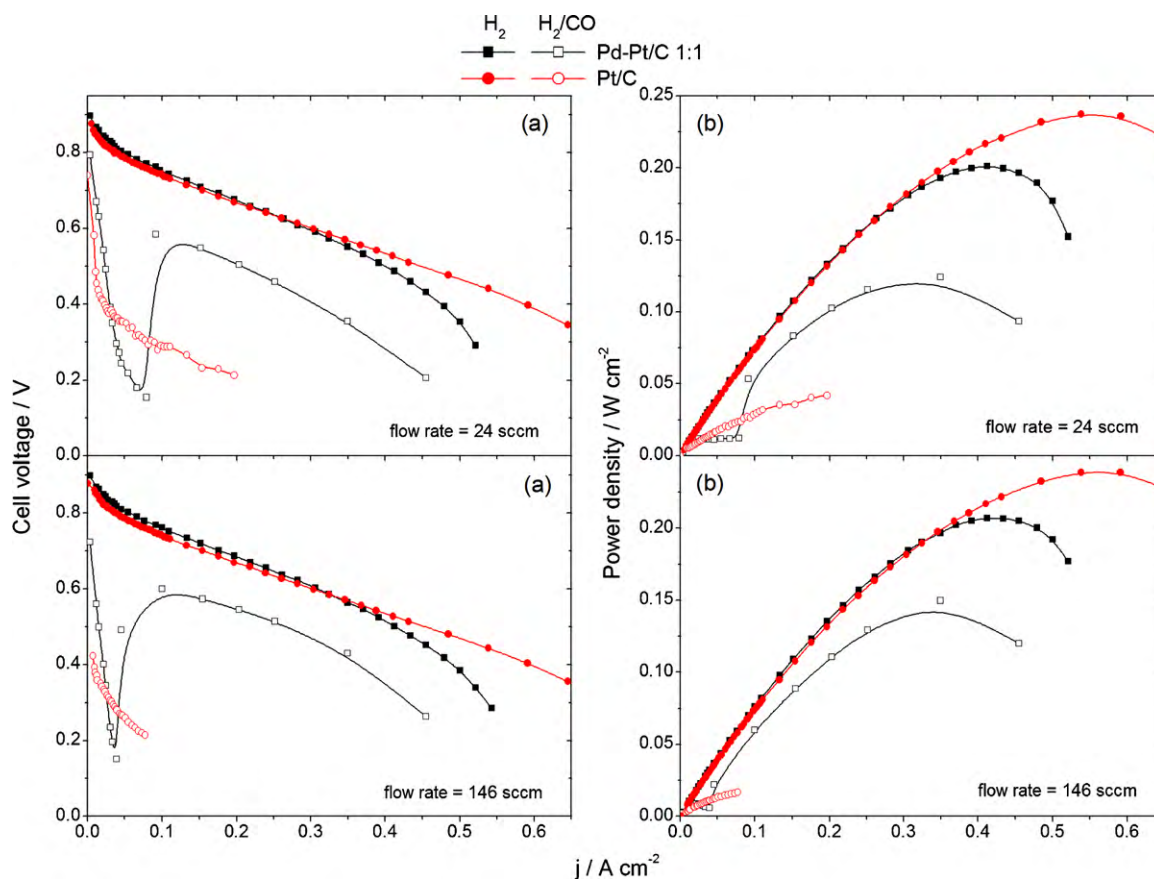E-mail address: varela@iqsc.usp.br (H. Varela).

Fig. 1. (a) Steady state polarization curves and (b) power density plots for the cell equipped with Pd–Pt/C and Pt/C as anode electrocatalysts when fed with H_2 or H_2/100 ppm CO at distinct flow rates.

impregnated powder was heat treated at 550 °C during 1 h under a hydrogen flow to reduce the Pd ions in order to form the electrocatalyst. The Pd:Pt atomic ratio was 1:1 as confirmed by EDS analysis. The obtained material was used as anode electrocatalyst, and the preparation of the electrode and MEA are described elsewhere [14]. The catalyst load was 0.4 mg Pt cm^{-2}. For comparison, a Pt/C anode was used with the same metal load than the Pd–Pt/C.

The electrochemical experiments were conducted on a single-cell hardware of 4.62 cm^2 of geometric area monitored by a working station from Fuel Cell Technologies University Test Station model. The steady state polarization curves were obtained in the galvanostatic mode by an electronic load from Amrel 6050 mounted in the test station and connected with a pc for data acquisition. The cathode was constantly feed with pure O_2 while in the anode with pure H_2 or H_2/100 ppm CO. The cell temperature was held constant at 30 °C. The hydrogen flow rate was changed between 24, 146 and 291 sccm in order to evaluate its effect over the oscillatory state. For obtaining the time-series with higher time resolution a multimeter Minipa ET-2615 was employed with 50 ms of sampling time. CO stripping voltammetry were conducted in order to access the CO oxidation potential for Pd–Pt/C and Pt/C. The working electrode (Pd–Pt/C or Pt/C) was previously adsorbed with CO for 10 min at 0.1 V vs. RHE at room temperature, than flushed with argon for 30 min to ensure complete CO removal from the system. After the pre-conditioning period the potential was swept at 10 mV s^{-1} and were recorded the first and second voltammetric profiles. The reference and counter electrode used is the Pt/C cathode fed with hydrogen flux during the whole experiment [3,4].

3. Results and discussion

Fig. 1 shows steady state polarization curves and the respective power density graphs registered at 30 °C for a PEMFC with Pd–Pd/C and Pt/C anodes when subjected to two distinct flow rates at the anodic compartment. Similar performances were observed between the anodes containing Pd–Pt/C and Pt/C when pure hydrogen was fed to the anodic chamber. Although the catalytic activity for the HOR in Pd is smaller than in Pt, Pd–Pt/C nanoparticles exhibit almost identical activity as pure Pt [4]. In contrast, Rau et al. [15] observed distinct activity towards the HOR on a Pd film electrode, and attributed it to a phase transition between α-Pd/H and β-Pd/H. When 100 ppm of CO is mixed in the hydrogen stream a severe performance decrease is observed for both Pt/C and Pd–Pt/C electrocatalysts. When the flow rate is increased, the potential loss becomes more pronounced at lower current densities, reflecting the increase in the CO partial pressure in the anode chamber for increased flow rates [16,17]. Independently on the flow, the voltage is higher for the cell with the Pd–Pt/C anode for most of the current range.

Garcia et al. observed that at higher temperatures Pd–Pt/C electrocatalysis exhibit higher CO tolerance [4]. Furthermore, the authors observed by CO striping voltammetry experiment that Pd containing materials have the CO oxidation peak shifted positively when compared to pure Pt. As the CO oxidative removal pathway is unfavored in Pd–Pt/C, the higher CO tolerance must be related to the energetics of the CO adsorption. The electronic effect discussed for bimetallic alloys is responsible for changing the CO adsorption energy by shifting the Pt 5d band structure [18]. Therefore, the lower overpotential for Pd–Pt/C for a fixed cell current can be
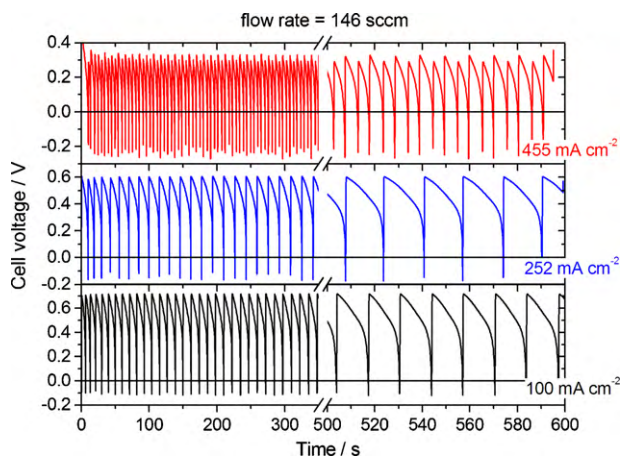
Fig. 2. Oscillatory time-series of the cell voltage for different cell currents. H_2/CO mixture admitted in the anodic chamber at 146 sccm. From bottom to top, the cell current density values are 100 mA cm^{-2} (black line), 252 mA cm^{-2} (blue line) and 455 mA cm^{-2} (red line). PEMFC with a Pd–Pt/C anode operated at 30 °C. (For interpretation of the references to color in this figure legend, the reader is referred to the web version of the article.)

due a reduced CO adsorption strength due the presence of Pd in the catalyst. Thus, while the electronic reorganization for Pt affects the CO coverage until a certain current threshold, above this value the CO oxidation becomes important. The CO tolerance mechanism on the PtRu/C electrocatalytic system was studied by Lopes and Ticianelli [19]. In their study the distinct action of the electronic effect and the bi-functional mechanisms were separated and their effects on the anode polarization profile discussed. The authors pointed out that the electronic effect shifts the beginning of the anode potential increase (equivalent to the sharp decrease in the cell potential observed here in Fig. 1a) and that the potential stabilization is directly related to the catalyst activity to oxidize CO to CO_2. The poor activity of Pd–Pt/C towards the electro-oxidation of CO promotes the potential increase. In summary, results presented in Fig. 1 evidence the effect of Pd on both adsorption and oxidation of carbon monoxide.

While for the Pt/C case the cell potential decreases monotonically for higher cell current, spontaneous potential oscillations emerge when the Pd–Pt/C anode is used, as anticipated by the discontinuity observed in Fig. 1a and b. The cell potential values plotted for current above the onset of the oscillations are a time average calculated by Eq. (1),

$$\langle V \rangle = \frac{1}{t_f - t_0} \int_{t_0}^{t_f} V(t)\, dt \tag{1}$$

It is clear that the time average power produced in the oscillatory state is much more elevated than that observed for the case of the Pt/C anode under non-oscillatory regime. Not only the power value but the current levels are four to five times higher during the oscillations.

Fig. 2 shows the oscillatory time-series for the cell voltages measured at different cell currents for an anodic flow rate of 146 sccm. It was discussed in the previous paragraph that instabilities may be used to enhance the energy production when the fuel contains CO levels. However, as clearly seen in Fig. 2, an inversion in the polarity of the fuel cell is also observed during the fast spike in the cell voltage. This is an important point and will be further discussed below. As observed in Fig. 2, from bottom to top, the increase in the cell current makes the oscillatory patterns more complex and promotes polarity inversions with increasing amplitudes.

As far as the oscillatory phenomena is concerned, this polarity inversion simply reflects the fast increase in the anode overpotential due to the dynamic of the oscillations with H_2/CO. Assuming that the cathode overpotential and the overall cell resistances remain constant, the voltage inversion is readily understood. For technological purposes, however, this inversion can be a hurdle from the point of view of power plant design. To benefit from the enhanced power generation with voltage inversion, one must couple another device that can delivery enough power with the same cell current and electric potential at least greater than the minimum oscillatory voltage in order to keep the total voltage of the system above zero. Therefore, the device must be carefully planned to meet this constraint in order to provide reliable electricity generation. Lu et al. [20] investigated a system that consists of two coupled cells for the promotion of CO removal from reformate in the oscillatory regime. They observed that serial type of electric connection results in an improved CO removal with higher power production. Polarity inversion on an individual cell was not previously observed due to smaller voltage amplitude intrinsic to the PtRu/C anode. In any case, this effect must be well evaluated.

Another issue that deserves comment is the high oscillation amplitude observed in Fig. 2. Although the minimum and maximum voltage values are displaced due to the cell current density, the oscillation amplitude amounts to about 0.80 V, which is a huge value when compared to formic acid and other small organic molecules that present oscillatory behavior on platinum surfaces [21,22]. Even oscillations that occur in PtRu electrodes do not go above 0.40 V in amplitude [5–7]. As previously reported [23], considerably large potential oscillations (amplitudes of about 0.60–0.70 V) have been observed for the oscillatory electrooxidation of formic acid on palladium. Thus, the large amplitudes observed here may be intrinsically related to Pd atoms and its catalytic activity towards CO electro-oxidation. One problem that may arise from this high amplitude is that the anode electrocatalyst is periodically submitted to elevated potential during the oscillations. Even though the time spent in this potential conditions is very small for each cycle, this could cause the catalyst degradation, by dissolution or by surface reconstruction, that eventually may alter the catalytic activity and thus modify its dynamic behavior towards the HOR in the presence of CO. In addition, the carbon support may also suffer from this elevated electrode potential, as its oxidation in the presence of Pt sites can begin at 0.80 V vs. SHE [24]. Therefore, this could also decrease the cell lifetime when operating under oscillatory regime.

In order to examine the oscillatory features observed on the Pd–Pt/C electrocatalyst, Figs. 3 and 4 show the anode overpotential for distinct cell current densities at two hydrogen flow rates: 24 sccm (Fig. 3) and 146 sccm (Fig. 4). Results for 291 sccm are not shown since they are very similar to those obtained for 146 sccm. The anode overpotential was calculated as shown in the literature [3–5],

$$\eta(j, t) = E_{H_2}(j) - E_{H_2/CO}(j, t) \tag{2}$$

which assumes that the cathode and cell resistances remain unaltered due the presence of CO in the anode.

From the oscillation patterns shown in Figs. 3 and 4 it can be readily observed the large oscillation amplitude for all cell currents and flow rates. This effect can be related to the low CO electrooxidation activity on Pd–Pt/C [4], as further discussed below. The effects of the hydrogen flow rate and cell current on the oscillatory frequency are summarized in Fig. 5a. As clearly seen, lower oscillation frequencies are observed for the lower flux studied (24 sccm), and this is a consequence of the lower CO concentration in the anodic chamber that accompanies the lower flow rate. This effect has been previously observed and discussed [17]. As pointed out by Datta and co-workers [5,7], the oscillation period is primarily
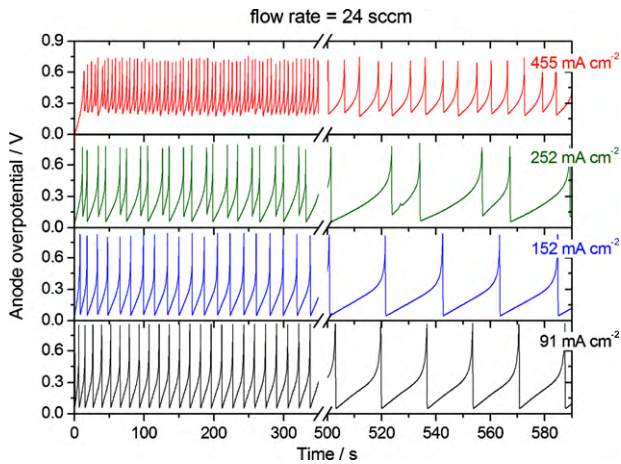
Fig. 3. Oscillatory time-series of the anode overpotential for different cell currents, with the H_2/CO mixture admitted in the anodic chamber at 24 sccm. From bottom to top, the cell current density values are 91 mA cm^{-2} (black line), 152 mA cm^{-2} (blue line), 252 mA cm^{-2} (green line) and 455 mA cm^{-2} (red line). PEMFC with a Pd–Pt/C anode operated at 30 °C. (For interpretation of the references to color in this figure legend, the reader is referred to the web version of the article.)
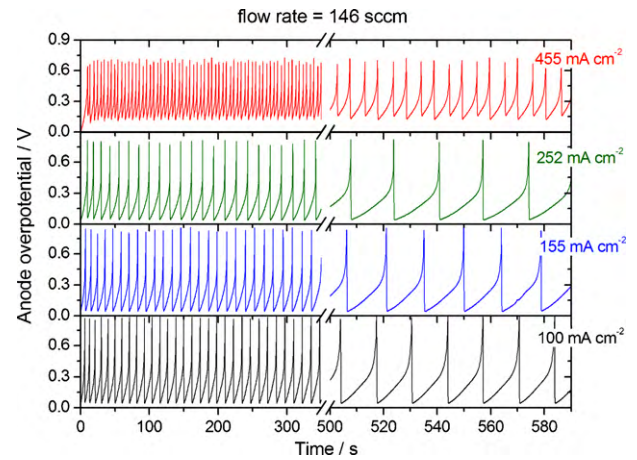
Fig. 4. Oscillatory time-series of the anode overpotential for different cell currents, with the H_2/CO mixture admitted in the anodic chamber at 146 sccm. From bottom to top, the cell current density values are 100 mA cm^{-2} (black line), 155 mA cm^{-2} (blue line), 252 mA cm^{-2} (green line) and 455 mA cm^{-2} (red line). PEMFC with a Pd–Pt/C anode operated at 30 °C. (For interpretation of the references to color in this figure legend, the reader is referred to the web version of the article.)

dictated by the CO adsorption period after its oxidative removal during the oscillation spikes. Thus, since the increase in the CO partial pressure increases the adsorption rate, the oscillation frequency will increase as well. However, we observe that the profile of the oscillation frequency vs. cell current is essentially the same for the higher flow rates. This is a consequence of the CO partial pressure saturation at higher flow rates, as it will be controlled by the initial CO content in the fuel stream and current density [16,17].

Independently on the flow rate, the current increase leads to a decrease in the oscillation frequency, which can be due to the small mean CO content inside the anodic chamber. Since under oscillatory regime carbon monoxide undergoes both adsorption and oxidation, the average CO partial pressure will depend on the cell current, as observed by Zhang et al. [7]. However, at higher cell currents the frequency starts to increase, and, eventually, a period doubling takes place. In Fig. 5a, the period-doubled patterns are characterized by two frequencies for a given cell current, see below.

Following the effect of the CO content, for low flow rate and high current densities, the hydrogen consumption rate will decrease the H_2 partial pressure, which will eventually concentrate the CO in the fuel stream. In summary, since the CO content has a major influence on the oscillation frequency, the trend observed here at low and high cell currents can be rationalized in terms of the CO partial pressure variation.

As already mentioned, period doubling might accompany the increase in the cell current at higher cell current. This period-two state can be characterized by two distinct amplitude cycles, namely small (S) and large (L) amplitude. This oscillatory feature can be recognized as having two oscillatory frequencies for the same flow rate and current density. For low gas flow rates, the period doubling starts at a low current density when compared to the higher flow rates, that only at 455 mA cm^{-2} shows the period-two state. Fig. 5b depicts the oscillatory amplitude vs. the subsequent time period, which helps us to understand the anode process in the period-two region. Overall, as we measured the oscillation amplitude vs. the time period that follows that potential spike, a clear correlation is observed: the smaller the oscillation amplitude, the longer the time required for the next poisoning step. As the potential amplitude
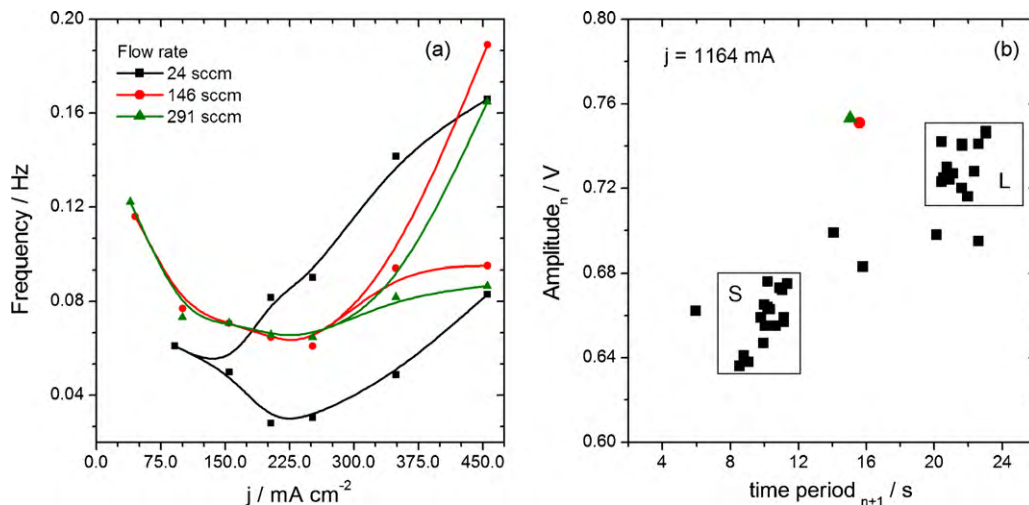

Fig. 5. (a) Oscillation frequency vs. cell current and (b) oscillation amplitude vs. time period at $j = 252$ mA cm^{-2} for three distinct hydrogen flow rate.
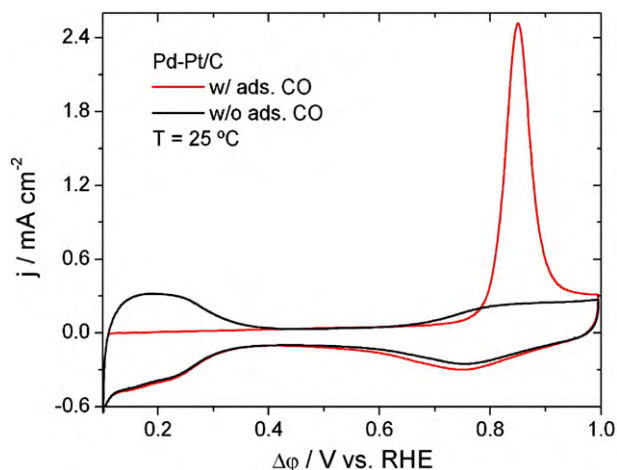
Fig. 6. CO stripping voltammetry of Pd–Pt/C catalyst. The red curve is the first voltammetric cycle after CO adsorption and flushing, while the black curve is the first cycle after the CO stripping.

reflect the ability to oxidize CO and thus, remove it from the surface, lower amplitude will leave more CO at the surface, shortening thus the next poisoning step. Accordingly, large amplitude cycles will be more effective in cleaning the electrode surface, and the following adsorption step will take longer. It should be emphasized that the CO adsorption process is characterized here by the time period between the oscillation cycles, or the time needed to reach the same potential value. So that, high CO coverage will result in a short subsequent time to completely poison the surface. Thus, the amplitude dictates the duration of the following adsorption step.

Since oscillations result of the combination of a variety of factors that are intrinsically entangled, the adsorption processes will also dictate the potential amplitude. The CO oxidation mechanism is believed to follow the Langmuir–Hinshelwood (L–H) pathway involving the reaction between adsorbed OH and adsorbed CO, with the rate determining step of the reaction corresponding to the formation of such OH species. Smaller oscillation amplitude makes the CO coverage higher, and this will reduce the free sites available for OH formation. Hence, with less OH formed on the surface, the CO oxidation process will occur efficiently only at elevated potentials. At high potentials, OH forms to a larger extent, which in turn reduces the CO coverage. A comparable delaying effect has been observed on numerical simulations of the L–H mechanism for the CO oxidation [25].

In the case of the oscillations observed when the PtRu/C anode is used, the amplitude does not go further than 0.40 V vs. RHE, which corresponds approximately to the CO stripping peak potential for this system at 25 °C [26]. For the Pt/C system, the peak potential is close to 0.70 V vs. RHE, and this value was used by Zhang et al. to explain why oscillatory dynamics are not observed in this electrocatalyst [7]. However, as observed from the results presented here, oscillations are not directly connected to the ability to form OH species or oxidize CO at low potentials. As found in the literature, the CO stripping peak potential for Pd containing materials are displaced to more positive values than for Pt, by about 0.20 V at 85 °C [4,27]. In this study we found that the CO stripping peak on Pd–Pt/C is close to 0.85 V vs. RHE at 25 °C, cf. Fig. 6. Another interesting feature is the appearance of the hydroxide region after 0.65 V vs. RHE, which may indicate that the water splitting reaction is just as active in this surface as on pure Pt. The oscillation amplitude goes near 0.8 V, and this is a good indicative that the CO stripping peak of a given material can be used to estimate the average oscillation amplitude. Therefore,

the emergence of such complex dynamics is not only conditioned to the CO oxidation process, but also the balance between the CO adsorption and oxidation rates is a key parameter to allow the emergence of spontaneous potential oscillations in this anodic material.

4. Conclusions

This paper reports the spontaneous emergence of potential oscillations in a PEMFC equipped with a Pd–Pt/C anode and fed with H_2/CO. The whole system was operated at 30 °C.

Oscillations were observed in a wide parameter range and are considerably different than those previously reported for a PEMFC with a PtRu/C anode. The influence of the cell current and fuel flow rate on the oscillations profile were evaluated. Overall, slow, relaxation-like oscillations characterize the dynamics. The mechanism underlying the oscillatory dynamics was rationalized in terms of the role of CO partial pressure and CO oxidation potential. These two aspects suffice to explain the general trends observed in the oscillations frequency and amplitude. The main aspects concerning the operation of a PEMFC under oscillatory regime was briefly discussed in terms of the higher average power output in the range of dynamic instabilities.

In spite of the considerable amount of comparable results available for half-cell experiments, oscillatory dynamics in a PEMFC have been reported only for devices using PtRu/C. Therefore, the present results extend the region in which kinetic instabilities are observed in practical systems.

References

[1] H.F. Oetjen, V.M. Schmidt, U. Stimming, F. Trila, J. Electrochem. Soc. 143 (1996) 3838–3842.
[2] S. Mukerjee, S.J. Lee, E.A. Ticianelli, J. McBreen, B.N. Grgur, N.M. Markovic, P.N. Ross, J.R. Giallombardo, E.S. De Castro, Electrochem. Solid-State Lett. 2 (1999) 12–15.
[3] L.G.S. Pereira, V.A. Paganin, E.A. Ticianelli, Electrochim. Acta 54 (2009) 1992–1998.
[4] A.C. Garcia, V.A. Paganin, E.A. Ticianelli, Electrochim. Acta 53 (2008) 4309–4315.
[5] J. Zhang, R. Datta, J. Electrochem. Soc. 149 (11) (2002) A1423–A1431.
[6] A. Mota, P.P. Lopes, E.A. Ticianelli, E.R. Gonzalez, H. Varela, J. Electrochem. Soc. 157 (9) (2010) B1301–B1304.
[7] J. Zhang, J.D. Fehribach, R. Datta, J. Electrochem. Soc. 151 (5) (2004) A689–A697.
[8] J. Zhang, R. Datta, J. Electrochem. Soc. 152 (6) (2005) A1180–A1187.
[9] K. Krischer, H. Varela, in: W. Vielstich, A. Lamm, H. Gasteiger (Eds.), Handbook of Fuel Cells, vol. 2, John Wiley & Sons, Chichester, 2003, pp. 679–701.
[10] R. Nagao, I.R. Epstein, E.R. Gonzalez, H. Varela, J. Phys. Chem. A 112 (2008) 4617–5462.
[11] S. Uhm, H.J. Lee, J. Lee, Phys. Chem. Chem. Phys. 11 (2009) 9326–9336.
[12] E. Boscheto, B.C. Batista, R.B. Lima, H. Varela, J. Electroanal. Chem. 642 (2010) 17–21.
[13] M. Carmo, V.A. Paganin, J.M. Rosolen, E.R. Gonzalez, J. Power Sources 142 (2005) 169–176.
[14] V.A. Paganin, E.A. Ticianelli, E.R. Gonzalez, J. Appl. Electrochem. 26 (1996) 297–304.
[15] M.S. Rau, P.M. Quaino, M.R. Gennero de Chialvo, A.C. Chialvo, Electrochem. Commun. 10 (2008) 208–212.
[16] J. Zhang, T. Thampan, R. Datta, J. Electrochem. Soc. 149 (6) (2002) A765–A772.
[17] J. Zhang, R. Datta, Electrochem. Solid-State Lett. 6 (1) (2003) A5–A8.
[18] E. Christoffersen, P. Liu, A. Ruban, H.L. Skriver, J.K. Norskov, J. Catal. 199 (2001) 123–131.
[19] P.P. Lopes, E.A. Ticianelli, J. Electroanal. Chem. 644 (2010) 110–116.
[20] H. Lu, L. Rihko-Struckman, R. Hanke-Rauschenbach, K. Sundmacher, Electrochim. Acta 54 (2009) 1184–1191.

[21] Y. Mukouyama, M. Kikuchi, G. Samjeské, M. Osawa, H. Okamoto, J. Phys. Chem. B 110 (2006) 11912–11917.
[22] E.A. Carbonio, R. Nagao, E.R. Gonzalez, H. Varela, Phys. Chem. Chem. Phys. 11 (2009) 665–670.
[23] M. Tian, B.E. Conway, J. Electroanal. Chem. 581 (2005) 176–189.
[24] K. Kinoshita, Carbon–Electrochemical and Physicochemical Properties, Wiley–Interscience, USA, 1988.
[25] P. Lopes, Electrocatalysis on Fuel Cells fed with Hydrogen, Verlag Dr. Müller, Saarbrücken, 2010.
[26] H.A. Gasteiger, N. Markovic, P.N. Ross, E.J. Cairns, J. Phys. Chem. 98 (1994) 617–625.
[27] D.C. Papageorgopoulos, M. Keijzer, J.B.J. Veldhius, F.A. de Bruijn, J. Electrochem. Soc. 149 (11) (2002) A1400–A1404.